

## Theory of two-phonon Raman spectrum of diamond\*

Riccardo Tubino<sup>†</sup> and Joseph L. Birman

*Physics Department, City College of the City University of New York, New York, New York 10031*

(Received 28 June 1976)

The Raman spectrum of diamond in the high-frequency part of the two-phonon region is investigated. An interpretation of the sharp line at the two-phonon cutoff as a simple overtone is supported in terms of a harmonic model for the potential and a bond polarizability approximation for the scattering Hamiltonian. Polarization features as well as the anomalous position and width of the peak are discussed and interpreted, giving general agreement between theory and experiment. A comparison is made with the Raman spectrum of silicon, and differences in the spectra are accounted for by a different behavior of the dispersion relation along  $\Delta$  for the two lattices, which has its origin in the greater angle-stiffness forces in diamond, ultimately due to greater covalency in diamond. A new set of critical points for the LO branch of diamond is also proposed.

### I. INTRODUCTION

The Raman spectrum of diamond has been carefully investigated experimentally in recent years. Accurate spectra have been obtained by Solin and Ramdas<sup>1</sup> in various scattering geometries, providing complete information on the three independent components of the scattering tensor as a function of the scattered frequency.

While vibrational spectra of other crystals having the diamond structure have been fully understood in terms of the available force-field models, some peculiar features in the Raman spectrum of diamond appear to remain controversial. Thus silicon and germanium seem<sup>2-4</sup> to have almost homologous vibrational properties—i.e., their dispersion curves, density of states, optical absorption, and Raman-scattering cross section almost overlap when considered as function of reduced frequency  $\omega/\omega_{\text{Ra}}$ . However, diamond exhibits its own spectral features.<sup>4</sup> In this paper, we will focus our attention on the region of the two-phonon cutoff, which, in the case of diamond, contains a sharp and polarized peak slightly above twice the frequency of the optical phonon. The origin of this feature is not in agreement with the usual critical-point analysis. The accompanying paper<sup>5</sup> reports new experimental results on the temperature dependence of the width and intensity of this feature, with which we shall compare our results.

The diamond-lattice space-group symmetry  $O_h^7$  contains two atoms in the primitive unit cell, giving rise to six phonon branches in the dispersion relation. At the  $\Gamma$  point, the three optical branches are triply degenerate and the corresponding phonons belong to the  $\Gamma_{25}^*$  irreducible representation. The one-phonon spectrum contains only one peak corresponding to the excitation of this optical phonon. The two-phonon Raman spec-

trum is more complex, since momentum conservation allows excitation of pairs with opposite momentum  $\pm q$  as long as other selection rules are also obeyed.

### II. RAMAN SCATTERING IN DIAMOND AND SILICON

The experimental two-phonon Raman scattering has recently been reported in diamond<sup>1,3</sup> and silicon.<sup>6</sup> We are particularly interested in the higher-frequency part of the two-phonon spectrum in the  $\Gamma_1^+$  polarization. In comparing diamond and silicon, it is noteworthy that a sharp polarized peak occurs near the two-phonon cutoff in diamond, while none is present in silicon. In the latter, the scattered intensity drops smoothly to zero as the scattered frequency shift approaches twice the Raman frequency  $2\omega_{\text{Ra}}$ .

Solin and Ramdas<sup>1</sup> stressed three points characterizing this "anomalous" peak at  $2667\text{ cm}^{-1}$ :

(i) The peak is anomalously sharp for a second-order feature and strongly polarized (it is always present for those scattering configurations in which the totally symmetric representation is excited). As a consequence of its  $\Gamma_1^+$  symmetry, this peak has not been observed in the infrared absorption.

(ii) The intensity of the peak is proportional to the excitation volume of the crystal.

(iii) The peak is shifted slightly above  $2\omega_{\text{Ra}}$ . Taking account of their available experimental resolution and the low intensity of second-order scattering, they estimated a shift of about  $2\text{ cm}^{-1}$ .

Washington and Cummins<sup>5</sup> report the peak to be shifted by  $3\text{ cm}^{-1}$  above  $2\omega_{\text{Ra}}$  at  $300\text{ K}$ , and to have a corrected width at half maximum of approximately  $4.2\text{ cm}^{-1}$ . They report, regarding this feature, "very little change in the shape, frequency shift, or relative intensity with respect to other second-order Raman features was observed as a function

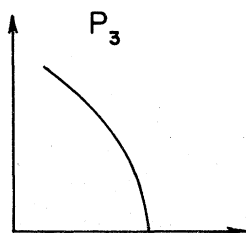


FIG. 1. Contribution to the density of states from a  $P_3$  critical point.

of temperature.”

It is natural to seek an explanation of the two-phonon spectrum in terms of the density of phonon states computed from phonon dispersion. Dispersion curves for silicon and diamond have been calculated using a shell model<sup>7</sup> and a valence force field.<sup>8</sup> These curves, obtained from strictly harmonic potentials, have seemed to indicate that the frequency of the optical phonon at  $\Gamma$  is the absolute maximum. Hence,  $\Gamma$  corresponds to a  $P_3$  critical point,<sup>9</sup> and the density of one-phonon states would go smoothly to zero at  $\omega_{Ra}$  (Fig. 1). The density of overtone states would likewise go smoothly to zero at  $2\omega_{Ra}$ . At first sight, an harmonic model seems to be inadequate to understand the Raman spectrum of diamond, while it accounts properly for the Raman spectrum of silicon and germanium.

Cohen and Ruvalds<sup>10</sup> interpreted the peak in diamond as evidence for the existence of a bound state in the two-phonon system. The explanation they proposed is as follows: the anharmonic phonon-phonon interactions in the Hamiltonian (which must be repulsive, in order to ensure stability of the bound state) split a state off the top of the two-phonon continuum, thus giving rise to a peak, whose separation from the continuum will be proportional to the strength of the anharmonic coupling. To account for a reported<sup>1</sup> shift of  $2\text{ cm}^{-1}$ , Cohen and Ruvalds made an estimate of the anharmonic potential energy  $V_4$  required. The magnitude of the anharmonic potential needed seemed in agreement with one semiempirical model for the potential.<sup>11</sup> More recent work indicates a rather significant disagreement between the needed magnitude and the magnitude of anharmonicity as estimated from thermal expansion and other measured quantities.<sup>12</sup>

Another drawback of this interpretation is that one would then expect bound states, with even greater shift from the continuum, to be observed in materials with known larger anharmonicity. In silicon and germanium, a number of experimental observations are consistent with the assumption that in these materials anharmonicity plays a more important role than in diamond. First, the half-width of the one-phonon line (which essentially measures the extent of the decay of optical phonons

through anharmonic interactions with other phonons) is  $1.2 \pm 0.2\text{ cm}^{-1}$  (corrected) for diamond<sup>5</sup> at  $300^\circ\text{K}$ , and  $3.4\text{ cm}^{-1}$  for silicon<sup>6</sup> at  $400^\circ\text{K}$ . Moreover, for silicon and germanium, the frequency of the  $\Lambda_1(A)$  branch along the  $\Gamma \rightarrow L$  symmetry direction calculated from an harmonic model (either valence<sup>8</sup> or shell model<sup>7</sup> is somewhat lower than the experimental neutron value. This does not happen for diamond. It is usually interpreted as evidence of larger anharmonicity in Si and Ge.

Despite these observations,<sup>12b</sup> which seem to indicate that anharmonic terms are of importance in the vibrational Hamiltonian of silicon and germanium, a two-phonon bound state has not been so far observed in these materials, even though two very accurate independent Raman studies on silicon have been recently reported.<sup>6,13</sup>

These considerations have motivated us to carefully examine the two-phonon spectrum of diamond within the harmonic framework. The intensity of the second-order scattering process (summation and overtone bands) as a function of the shifted frequency can be written

$$I_{\alpha\beta\gamma\delta}^{\text{II}}(\omega) = \int_q \sum_j \sum_{j'} H_{jj'}^{\alpha\beta\gamma\delta}(q) [1 + n(qj) + n(qj')] \times \delta(\omega - \omega(q, j) - \omega(q, j')) dq, \quad (1)$$

where  $I_{\alpha\beta\gamma\delta}^{\text{II}}$  is a component of the second-order Raman tensor,<sup>14</sup>  $n(qj)$  is the occupation number (using Bose statistics),  $q$  is the phonon wave vector, and  $H_{jj'}^{\alpha\beta\gamma\delta}$  is the Hamiltonian which couples the phonons  $j$  and  $j'$  of opposite wave vector  $\pm q$  with the radiation.

If the frequency of incident radiation is far from the frequency of any electronic excitation of the crystal, then, within the framework of polarizability theory,<sup>15</sup> the Hamiltonian is a bilinear form in the second derivatives of the crystal polarizability with respect to the normal coordinates  $Q$  of the two phonons involved:

$$H_{jj'}^{\alpha\beta\gamma\delta}(q) \propto \left( \frac{\partial^2 P_{\alpha\beta}}{\partial Q(q, j) \partial Q(q, j')} \right)_0 \left( \frac{\partial^2 P_{\gamma\delta}}{\partial Q(q, j) \partial Q(q, j')} \right)_0^* \quad (2)$$

Since crystals having diamond structure are strongly covalent and their electrons can be thought of as localized in highly directional chemical bonds, a model was proposed by one of the authors in which the crystal polarizability is expressed as a sum of individual bond contributions. Details of this model for the Hamiltonian and the valence force field used for this calculation can be found elsewhere,<sup>16,8</sup> together with some earlier results for the phonon dispersion in diamond.

From that calculation we observe that (i) a sim-

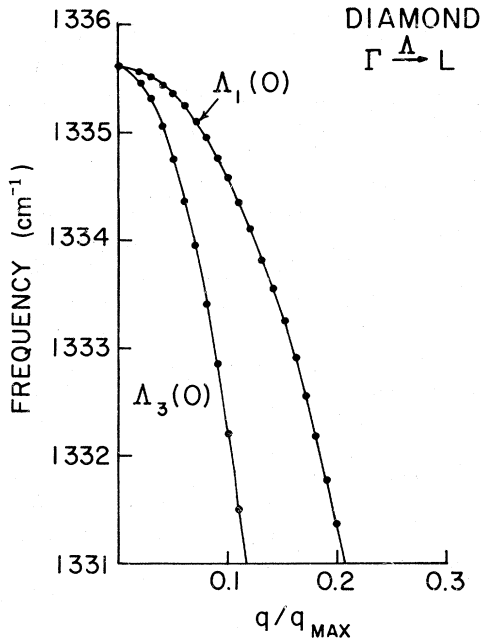


FIG. 2. Detail of dispersion curves for diamond around  $\Gamma$ : Direction  $\Gamma\Delta L$ .

ple two-phonon density of states (summation and overtone) reproduces the positions of the observed peaks rather well but does not properly account for relative intensities in general (see Fig. 2 of Ref. 16); (ii) in polarizations for which the  $\Gamma_1^+$  component of the spectrum is excited, a fairly good approximation to the Raman intensity versus frequency *is* provided simply by the density of overtones (In cases with several polarizations simultaneously present,  $\Gamma_1^+$  is quantitatively more important than  $\Gamma_{12}^+$  and  $\Gamma_{25}^+$  and masks these latter components.); (iii) in any scattering geometry with  $\Gamma_1^+$  excited, the sharp peak at the two-phonon cutoff occurs in the calculation in agreement with experiment.

Neglecting thermal factors which are of no importance for the present analysis, Eq. (1) can be written

$$I_{\alpha\beta\gamma\delta}^{\text{II}}(\omega) \propto \sum_{jj'} \int_{\Omega(q)} H_{jj'}^{\alpha\beta\gamma\delta}(q) \delta(\omega - \Omega(q)) \frac{dq}{d\Omega} d\Omega, \quad (3)$$

where  $\Omega(q) = \omega(q, j) + \omega(q, j')$ . By using the properties of the Dirac function,

$$I_{\alpha\beta\gamma\delta}^{\text{II}}(\omega) \propto H^{\alpha\beta\gamma\delta}(\omega) G(\omega), \quad (4)$$

where  $G(\omega)$  is the two phonon density of states at  $\omega$  and  $H^{\alpha\beta\gamma\delta}(\omega)$  is the "coupling Hamiltonian" expressed as a function of frequency [as defined by Eq. (3), branch indices  $j$  and  $j'$ , and wave vector

$q$  define a frequency  $\omega$ ].

From Eq. (4), it follows that in the vicinity of  $2\omega_{\text{Ra}}$  the intensity of the scattered phonons should mimic the two-phonon density of states. If the latter has a  $P_3$ -type critical point at  $2\omega_{\text{Ra}}$ , then we cannot explain a peak near  $2\omega_{\text{Ra}}$ , *except* in the improbable circumstance that  $H(\omega)$  becomes unexpectedly singular at  $2\omega_{\text{Ra}}$ , and overcompensates the vanishing density of overtone states.

### III. PHONON DISPERSION IN DIAMOND AND SILICON

A way out of this dilemma was suggested by the conjecture of Uchinokura *et al.*<sup>13</sup> that one of the optical branches has its absolute maximum not at  $\Gamma$ . To test this proposal we decided to carefully reexamine the phonon dispersion in diamond and silicon along the main symmetry directions, using the valence force field potential of Ref. 8. A brief report of this work was given earlier<sup>17</sup> and the present report gives more details of the calculation.

Results for diamond and silicon are given in Figs. 2-5. A significant difference in the harmonic lattice dynamics of diamond and silicon is evident along the  $\Gamma\Delta X$  symmetry direction. While in silicon, both the TO and LO branches sharply drop in frequency as  $q$  becomes finite, in diamond, the LO branch slowly increases in frequency, reaching its absolute maximum along the  $\Delta$  direction.

Coherent neutron data on diamond,<sup>18</sup> from which the parameters of our model have been obtained,

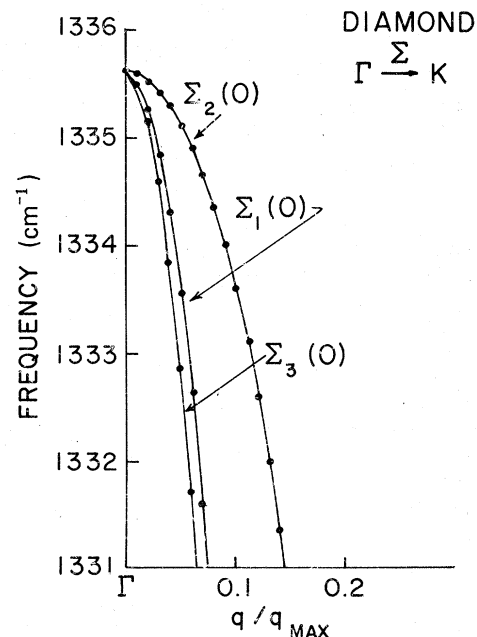


FIG. 3. Detail of dispersion curves for diamond around  $\Gamma$ : Direction  $\Gamma\Sigma K$ .

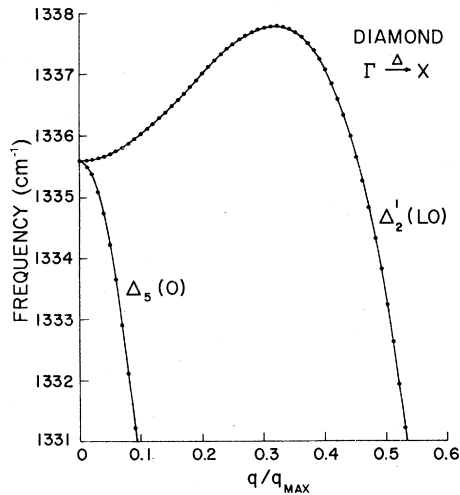


FIG. 4. Detail of dispersion curves for diamond around  $\Gamma$ : Direction  $\Gamma \rightarrow X$ .

are not available for the LO branch along this symmetry direction. More recent data by Peckham<sup>19</sup> are consistent with the calculated shallow maximum, but in this high-frequency region of the spectrum, neutron data are not very accurate. Since the model fits the available experimental data throughout the Brillouin zone, we believe the predicted behavior of the LO branch is correct. In order to classify the new critical point at  $\Gamma$ , Phillips's analysis<sup>9</sup> can be used. Following Phillips, we count the number of separate frequency sectors in the neighborhood of the critical point in which  $\omega - \omega_0 > 0$  ( $\omega_0$  being the frequency at the critical point) or  $\omega - \omega_0 < 0$ . A positive (or negative) sector is a solid angle, taken with the critical point as apex for which the difference  $\omega - \omega_0$  is everywhere positive (or negative). In Fig. 6, a section for  $q_x = 0$  of the irreducible element of the Brillouin zone for diamond is shown. The dashed area shows values of  $q$  for which the LO branch has a frequency higher than the optical phonon. Phillips showed that separate sectors are possible only in the directions  $\Delta \equiv \langle 100 \rangle$ ,  $\Sigma \equiv \langle 110 \rangle$ ,  $\Lambda \equiv \langle 111 \rangle$ , and along a general direction for which two components of the wave vector are the same  $G$ . From the various possible combinations of positive and negative sectors, a critical point can be classified. In our case, we have for the alternation of signs

$$(\Delta +; \Sigma -; \Lambda -; G -),$$

and therefore the  $\Gamma$  point in diamond can be classified as  $\delta_2$  point. (A critical point analysis of crystals with the diamond structure was reported earlier by Bilz *et al.*<sup>2</sup> on the basis of infrared absorption studies of diamond. Since no combination band has a frequency higher than the two-phonon

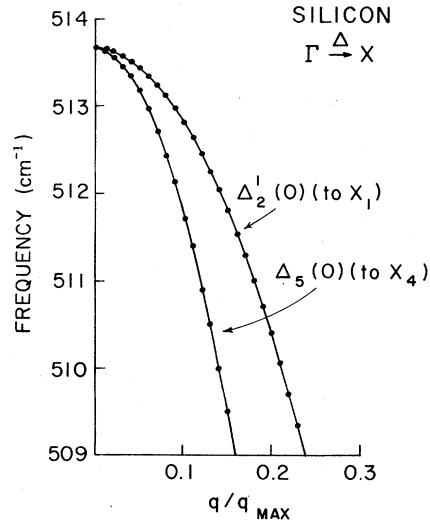


FIG. 5. Detail of dispersion curves for silicon around  $\Gamma$ : Direction  $\Gamma \rightarrow X$ .

cutoff, the infrared spectrum is unable to show the true structure of the LO branch.) On the basis of the Raman spectrum and of our results, critical points for the LO branch are as follows:

	$\Gamma$	$X$	$L$	$W$	$\Sigma$	$\Delta$
for silicon	$P_3$	$P_2$	$P_2$	$P_0$	$P_1$	
for diamond	$\delta_2$	$P_2$	$P_2$	$P_0$	$P_1$	$P_3$

We shall utilize these assignments in the interpretation of the Raman spectrum for  $\Gamma_1^+$  polarization, where the scattering is mainly due to the density of overtones (i.e., the one-phonon density of states "doubled" up to  $2\omega_{Ra}$ ). The different structure of critical points for diamond and silicon gives rise to a different behavior in the overtone density of states and therefore in the spectrum.

We previously reported (Figs. 2 and 3 of Ref. 17) the overtone density of states in diamond and silicon. Comparing these with the experimental spectra of Refs. 2 and 5, we note that for silicon the experimental spectrum has been obtained with a much lower resolution ( $5 \text{ cm}^{-1}$ ) than the calculated

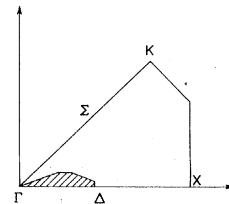


FIG. 6.  $xy$  section of the irreducible element of the Brillouin zone in diamond showing  $q$  values for which the frequency of LO branch is higher than at  $\Gamma$ .

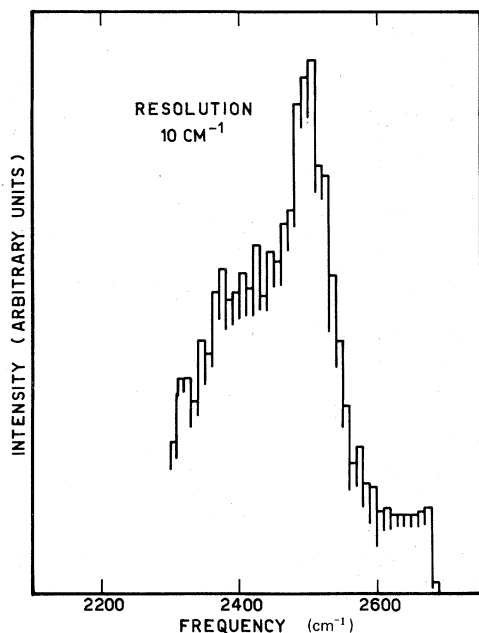


FIG. 7. Overtone density of states (high-frequency section) for diamond (resolution  $10 \text{ cm}^{-1}$ ).

histogram ( $1 \text{ cm}^{-1}$ ); some lack of agreement in the fine structure has to be expected. In particular, the two calculated sharp peaks correspond to smoothed out kinks in the experimental spectrum. Apart from that, the agreement between calculation and experiment is very good. For silicon, the expected  $P_3$  singularity is found at the cutoff of

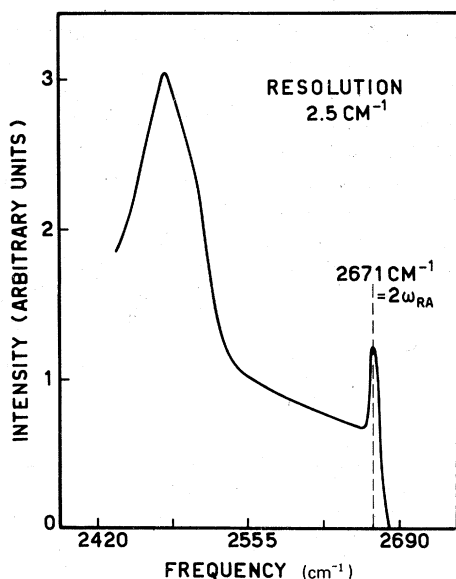


FIG. 8. Overtone density of states (high-frequency section) for diamond (resolution  $2.6 \text{ cm}^{-1}$ ).

$2\omega_{\text{RA}}$ .

For diamond the sharp peak at  $2667 \text{ cm}^{-1}$  is easily identified with a corresponding sharp kink in the density of the states due to the  $\delta_2$  point. Since we are using an harmonic model, the calculated feature is an overtone which occurs at  $2\omega_{\text{RA}}$  and is not displaced from twice the calculated Raman frequency ( $1335.6 \text{ cm}^{-1}$ ). We note, however, that according to our results, the density of overtone states in diamond goes to zero,  $5 \text{ cm}^{-1}$  above  $2\omega_{\text{RA}}$  and therefore "bound pair" states in diamond cannot occur within this frequency shift. Our provisional interpretation of the measured  $3\text{-cm}^{-1}$  shift of the overtone is that it is due to anharmonic effects which would displace the apparent peak from simply double the one-phonon (Raman) frequency. In Ref. 8, an earlier calculated density of states for diamond and silicon using the same potential model was reported. In this earlier work, the histogram resolution ( $10 \text{ cm}^{-1}$  for diamond and  $5 \text{ cm}^{-1}$  for silicon) is insufficient to show fine structure.

More accurate calculations were possible in the present work, using an interpolation procedure for obtaining the density of states. The effect of increasing the resolution of the calculation is shown (for diamond) in Figs. 7-9. It can be noted that at the level of  $10\text{-cm}^{-1}$  resolution no "anomalous" peak near  $2\omega_{\text{RA}}$  can be seen, while for a finer grid, the peak is clearly seen. From the calculations of Fig. 9, the calculated halfwidth of the peak can be obtained as  $5\text{-}6 \text{ cm}^{-1}$ .

Summarizing, we believe that the "anomalous" Raman peak found in the two-phonon Raman spectrum of diamond is simply due to the scattering from LO overtone states at  $\Gamma$  and along the  $\Delta$  sym-

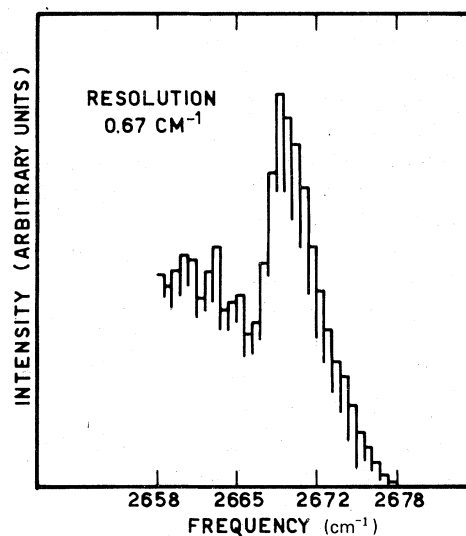


FIG. 9. Overtone density of states (high-frequency section) for diamond (resolution  $0.67 \text{ cm}^{-1}$ ).

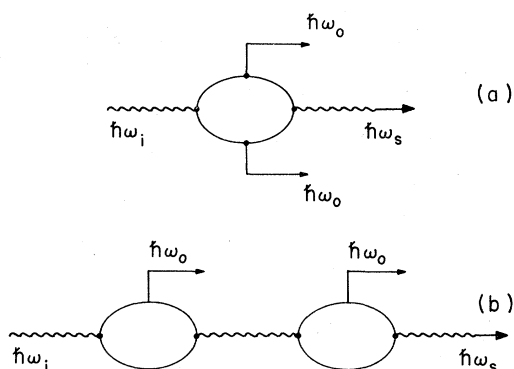


FIG. 10. Schematic diagrams showing (a) one-step and (b) two-step scattering processes.

metry direction. This is consistent with the observed shape of the peak and with the polarization features: mainly,  $\Gamma_1^+$  symmetry, but also some weak components belonging to other symmetries ( $\Gamma_{25}^+ \otimes \Gamma_{25}^+$ )<sub>(2)</sub> =  $\Gamma_1^+ \oplus \Gamma_{12}^+ \oplus \Gamma_{25}^+$ . Anharmonic corrections may account for its slight frequency shift. Moreover, the present model predicts that the intensity of the peak should be proportional to the excitation volume as in other parts of the spectrum and not to the square of the volume, since the peak is due to a regular one-step second-order process [Fig. 10(a)], and not to "two successive first-order Raman scatterings at the zone center."<sup>20</sup> [Fig. 10(b)]. Other evidence supporting our interpretations are as follows.

*a. T-dependence of the peak intensity.* An  $(\eta_{\omega T} + 1)$  temperature dependence for the Raman intensity of the regular overtone spectrum is expected (diamond being an insulator). An intensity ratio of 1.003 ( $T_1 = 300^\circ\text{K}$  and  $T_2 = 23^\circ\text{K}$ ) for the zone center overtone is calculated, in agreement with no observed<sup>5</sup> appreciable change in intensity for the peak at the two-phonon cutoff.

*b. One-phonon defect activated infrared spectrum.* Indirect evidence of an overbending of the LO phonons may be found in the two-phonon defect induced infrared spectrum of diamond, recently reported.<sup>21</sup> Among the *B* features of the spectrum (and weakly also among the *A* features), a sharp absorption at  $1332\text{ cm}^{-1}$  is found due to the Raman phonons excited by radiation damage products. Since common features to the *A* and *B* forms usually have their origin in high densities of band modes, it seems possible to relate this absorption to the kink shown in the calculated density of states at the cutoff.

#### IV. MICROSCOPIC INTERPRETATION

We should try now to understand the phonon dispersion in diamond, in terms of its lattice dynam-

ics and forces acting in the crystal. For crystals having the diamond structure, the dispersion relation for the LO branch along the  $\Delta$  direction can be written analytically,

$$M\omega_{\text{LO}}^2 = \frac{1}{2}M\omega_{\text{Ra}}^2 + 8\mu(1 - \cos\pi q) + 4\alpha \cos(\frac{1}{2}\pi q), \quad (5)$$

where  $M$  is the carbon mass,  $\omega_{\text{Ra}}$  is the Raman frequency at the zone center,  $q$  is the wave vector (taking values along  $\Delta$ ), and  $\alpha$  and  $\mu$  are general Born force constants for first- and second-neighbor interaction (Table I). The condition for a maximum in this curve is

$$8\mu \sin(\frac{1}{2}\pi q) / \cos(\frac{1}{2}\pi q) - \alpha \sin(\frac{1}{2}\pi q) = 0, \quad (6)$$

which leads to a solution  $q=0$  for the  $\Gamma$  point, and also for a point defined by the equation

$$q = (2/\pi) \arccos(\alpha/8\mu). \quad (7)$$

If  $8\mu/\alpha < 1$ , the dispersion curve displays a monotonic decreasing behavior, otherwise a maximum is expected. We can express the Born force constants in terms of valence force constants

$$\alpha = \frac{1}{3}(2K_R - 2F_R - 8\sqrt{2} F_{\text{RA}}/R + 8H_\Lambda/R^2), \quad (8)$$

$$\mu = \frac{1}{6}(2F_R + 2H_\Lambda/R^2 + 2\sqrt{2} F_{\text{RA}}/R - 6F_\Lambda''/R^2). \quad (9)$$

Using values for the parameters obtained for our model,<sup>8</sup> we find  $8\mu/\alpha = 1.098$  for diamond,  $8\mu/\alpha = 0.249$  for silicon, and  $8\mu/\alpha = 0.568$  for germanium.

The anomalous Raman scattering in diamond is then related to some critical ratio of second- to first-neighbor interaction forces. If the ratio  $8\mu/\alpha$  increases to greater than one, the frequency maximum shifts towards the edge of the edge of the Brillouin zone. Since the second-neighbor force constant  $\mu$  is mainly connected with bending forces and their interactions, a more marked angular character appears to be peculiar to forces acting in the diamond lattice. The situation is similar, regarding the ordering of branches at  $X$  point. For silicon and germanium, the energy of  $X_4(\text{TO})$  phonon is higher than the energy for  $X_1(\text{LO, LA})$ , but the opposite occurs for diamond. Like the overbending along  $\Delta$  in diamond, the branch interchanges at  $X$  are not required by symmetry, but are a consequence of particular forces acting in the lattice.

TABLE I. Interatomic-force-constant matrices for general forces (first and second neighbors).

$\alpha$	$\beta$	$\beta$	$\mu$	$\nu$	$\delta$
$\beta$	$\alpha$	$\beta$	$\nu$	$\mu$	$\delta$
$\beta$	$\beta$	$\alpha$	$\delta$	$\delta$	$\lambda$

## V. CONCLUSION

The present work provides a simple and, we believe, persuasive explanation of the origin of the sharp peak near the two-phonon cutoff observed in the Raman spectrum of diamond.

A harmonic valence force field for the potential, and a bond polarizability model for the Raman scattering account for the existence of a sharp peak near the two-phonon cutoff, and give good agreement with experiment<sup>1,5</sup> regarding the width of the peak, its relative intensity, and polarization.<sup>16</sup> The shift of the location of the maximum of the peak by  $3\text{ cm}^{-1}$  from the position of  $2\omega_{\text{Ra}}$  (approximate

mately  $2669\text{ cm}^{-1}$ , in the accompanying paper) is not given by our theory. We surmise that proper inclusion of anharmonicity in our model will produce this small shift, while retaining the major feature of our interpretation—namely, that the peak is due to an “unbound” overtone. We are persuaded that it is not necessary to invoke the hypothesis of a two-phonon Raman scattering feature in diamond.

## ACKNOWLEDGMENTS

We thank Dr. M. A. Washington and Professor H. Z. Cummins for discussions.

\*Supported in part by AROD Grant No. DAHCO4-75-G-0052, NSF Grant No. DMR74-21991 A01, and FRAP-CUNY Grant No. 10753N.

†Permanent address: Istituto di Chimica delle Macromolecole del CNR, Via Alfonso Corti 12, 20133 Milano, Italy.

<sup>1</sup>S. A. Solin and A. K. Ramdas, *Phys. Rev. B* **1**, 1687 (1970).

<sup>2</sup>H. Bilz, R. Geick, and K. F. Renk, in *Lattice Dynamics*, edited by R. F. Wallis (Pergamon, London, 1965), p. 355.

<sup>3</sup>T. J. Kucher, *Fiz. Tverd. Tela (Leningrad)* **4**, 2385 (1962) [*Sov. Phys. Solid State* **4**, 1747 (1963)].

<sup>4</sup>F. A. Johnson and R. Loudon, *Proc. R. Soc. A* **281**, 274 (1964).

<sup>5</sup>M. A. Washington and H. Z. Cummins, preceding paper, *Phys. Rev. B* **15**, 5840 (1977).

<sup>6</sup>P. A. Temple and C. E. Hathaway, *Phys. Rev. B* **7**, 3685 (1973).

<sup>7</sup>G. Dolling and R. A. Cowley, *Proc. Phys. Soc. Lond.* **88**, 463 (1966).

<sup>8</sup>R. Tubino, L. Piseri, and G. Zerbi, *J. Chem. Phys.* **56**, 1022 (1972).

<sup>9</sup>J. C. Phillips, *Phys. Rev.* **104**, 1263 (1956).

<sup>10</sup>M. H. Cohen and J. Ruvalds, *Phys. Rev. Lett.* **23**, 1378 (1969).

<sup>11</sup>R. F. Borkman and R. G. Parr, *J. Chem. Phys.* **48**,

1116 (1968).

<sup>12</sup>(a) A. A. Maradudin, in *Phonons*, edited by M. Nusi-movici (Flammarion, Paris, 1971), p. 427; (b) C. H. Wu and J. L. Birman, *J. Phys. Chem. Solids* **36**, 305 (1975).

<sup>13</sup>K. Uchinokura, T. Sekine, and E. Matsuura, *J. Phys. Chem. Solids* **35**, 17 (1974).

<sup>14</sup>R. A. Cowley, in *The Raman Effect*, edited by A. Anderson (Marcel Dekker, New York, 1971).

<sup>15</sup>G. Placzek, *Max Handbuch der Radiologie*, 2nd ed. (Academische Verlagsgesellschaft, Leipzig, 1934), p. 209.

<sup>16</sup>R. Tubino and L. Piseri, *Phys. Rev. B* **11**, 5145 (1975).

<sup>17</sup>R. Tubino and J. L. Birman, *Phys. Rev. Lett.* **35**, 670 (1975).

<sup>18</sup>J. L. Warren, J. L. Yarnell, G. Dolling, and R. A. Cowley, *Phys. Rev.* **158**, 805 (1967).

<sup>19</sup>G. Peckham, *Solid State Commun.* **5**, 311 (1967), and private communication.

<sup>20</sup>R. Loudon, *Adv. Phys.* **13**, 423 (1964).

<sup>21</sup>G. Davies, *Proceedings of the International Conference on Phonons, Rennes* (Flammarion, Paris, 1971), p. 382; also, for electric field effect on infrared absorption, see J. Angress *et al.*, *ibid.*, p. 459. Although resolution was insufficient to be decisive, this experiment also is suggestive of our interpretation.